



HAL
open science

Influence of the stacking sequence and crack velocity on fracture toughness of woven composite laminates in mode I

Pablo Navarro, Julien Aubry, Florian Pascal, Steven Marguet, Jean-François Ferrero, Olivier Dorival

► To cite this version:

Pablo Navarro, Julien Aubry, Florian Pascal, Steven Marguet, Jean-François Ferrero, et al.. Influence of the stacking sequence and crack velocity on fracture toughness of woven composite laminates in mode I. *Engineering Fracture Mechanics*, 2014, 131, pp.340-348. 10.1016/j.engfracmech.2014.08.010 . hal-01183154

HAL Id: hal-01183154

<https://hal.science/hal-01183154>

Submitted on 7 Jun 2019

HAL is a multi-disciplinary open access archive for the deposit and dissemination of scientific research documents, whether they are published or not. The documents may come from teaching and research institutions in France or abroad, or from public or private research centers.

L'archive ouverte pluridisciplinaire **HAL**, est destinée au dépôt et à la diffusion de documents scientifiques de niveau recherche, publiés ou non, émanant des établissements d'enseignement et de recherche français ou étrangers, des laboratoires publics ou privés.

Influence of the stacking sequence and crack velocity on fracture toughness of woven composite laminates in mode I

P. Navarro ^a, J. Aubry ^a, F. Pascal ^a, S. Marguet ^a, J.F. Ferrero ^{a,*}, O. Dorival ^b

^a Université de Toulouse; INSA, UPS, Mines Albi, ISAE; ICA (Institut Clément Ader), 10 Avenue Edouard Belin, BP54032, 31055 Toulouse Cedex 4, France

^b LMT-Cachan (ENS Cachan/CNRS/PRES Univ Sud Paris), 61 av; President Wilson, Cachan 94235, France

Woven composites are well-known for their good transverse properties and for their high fracture toughness. The damage mechanisms leading to delamination in woven composites are identified in mode I. The influence of several parameters, including the draping sequence and the fiber/matrix interface on the fracture toughness of woven composite laminates is studied. Pure mode I tests are carried out on several carbon/epoxy and glass/epoxy woven composites configurations and the differences observed are discussed from a fractographic point of view. A novel experimental method is designed to perform dynamic pure mode I tests. The study illustrates the high fracture toughness of the composites made of woven fabrics as well as the influence of the orientation of the plies, the nature of the fibers and the addition of an adhesive film on the fracture toughness in mode I. The dynamic tests prove that, on the configurations tested and for crack velocities up to 100 m/s, the crack propagation velocity has a limited effect on the value of G_{Ic} .

1. Introduction

The laminate structure of composites makes delamination a critical damage mechanism at the interfaces between plies. Delamination may reduce the in-plane strength and stiffness and can lead to the failure of the composite structure [1]. Study of the fracture toughness of composite is thus fundamental for the characterization of composites.

In laminates made from unidirectional plies, cracks can propagate between plies and cross a ply through the matrix [2].

Woven fabrics can be used to block the intra-ply crack propagation. Indeed, the entanglement of the warp and weft tows prevents the crack from crossing the plies. Generally, woven composites show higher fracture toughness compared with unidirectional composites as shown by early studies of Funk and Deaton [3]. The authors have quantified the greater values of G_{Ic} for carbon/epoxy woven fabrics compared to carbon/epoxy unidirectional tape. Values of 300–500 J m⁻² were recorded for the woven fabrics, to be compared with the critical energy release rate of 100 J m⁻² for the unidirectional composite.

This difference is also explained by the intrinsic roughness of woven fabrics that increases the surface to be separated [4]. Kim and Sham [5] also explain the greater toughness by the alternation of warp and weft tows. When the crack propagates in the warp direction, the fibers parallel to the crack propagation tend to speed up the crack, whereas for the weft tows, the fibers are perpendicular to the crack propagation and tend to slow down the crack [6]. This effect is also found in unidirectional laminates where delamination off the axis of the fibers requires more energy [7].

* Corresponding author.

Nomenclature

P	load
δ	opening
B	width of the specimen
a	crack length
Δa	corrective term
F	corrective term
N	corrective term
G_{Ic}	energy release rate

Woven fabrics are not affected by fiber bridging the same way unidirectional laminates are. The entanglement of the tows generally prevents the fibers from being torn off from the composite surface [4]. However Alif et al. [8] have shown that fiber bridging in woven fabrics can still play an important role in dissipating energy. For this type of composites, fibers from the warp direction can break between two tows in the weft direction and be torn off the composite surface. This phenomenon is particularly predominant in twill and satin weave pattern compared to plain weave pattern, where the distance between two weft tows prevents fibers to be pulled out [8].

Dynamic crack propagation has been mainly investigated on unidirectional composites. Experimental set-ups include modified wedge tests on Hopkinson bars [9,10], specific rigs for high-speed hydraulic machines [11] or drop weight towers [12]. All of these studies have established that measuring a dynamic fracture toughness in mode I is complex, either for measurements problems considering the velocity of the phenomena, or because the inertia of the specific rigs makes it impossible to reach a steady crack propagation state before the complete failure of the specimen. Guo and Sun [13] have worked on a modified experiment that consists in placing an adhesive film right after the pre-crack. This allows charging the specimen before the crack propagates and produces crack velocities up to 200 m s^{-1} , with close to quasistatic loading rates.

Damage mechanisms during delamination of woven fabrics are thus known up to a certain point. However most articles study the delamination of woven fabrics in the warp or weft directions. In this paper, we present an experimental study in pure mode I of the influence of the orientation of the woven fabric plies, of the material nature and of crack propagation speed. A fractographic study is carried out on each configuration to bring to light the damage mechanisms leading to delamination and to relate the delaminated surfaces obtained with the value of the fracture toughness of the composite.

2. Experimental procedure

2.1. Materials and specimen manufacture

Hexcel 913/45%/7781 satin weave glass fabrics and Hexcel 913/45%/G963 satin weave carbon fabrics are used to manufacture the specimens. Both fabrics are 0.3 mm thick pre-impregnated plies. The adhesive used in this study is a 0.1 mm thick Hysol EA 9686 unreinforced epoxy film.

For each configuration tested, a 12 plies-thick panel is manufactured using a hydraulic heating press. A $40 \mu\text{m}$ thick PTFE film is placed at mid-thickness to initiate the delamination. The stacking sequence of each configuration is chosen so that the stiffness of the two arms of the specimen is equal and so that the bending of the arms does not produce torsion, as advised by several papers [14,15]. Each panel is cut using a diamond saw into specimens of length 170 mm and width 20 mm.

The stacking sequences for each configuration are given in Table 1 where C stands for a ply of carbon woven fabric, G for a ply of glass woven fabric and *adh.* stands for a ply of adhesive. For each interface, the numbers given in subscript indicates the angle between the warp direction and the crack propagation direction. Four specimens are tested for each configuration to account for statistic distribution.

Table 1
Stacking sequence of the configurations tested.

Influence tested	Studied interface	Stacking sequence
Stacking sequence	C_0/C_0	$(C_0)_6/(C_0)_6$
	C_0/C_{45}	$(C_0)_4 C_{45} C_0/C_{45} (C_0)_5$
	C_{45}/C_{45}	$(C_0)_5 C_{45}/C_{45} (C_0)_5$
Material nature	G_0/G_0	$(C_0)_5 G_0/G_0 (C_0)_5$
	C_0/G_0	$(C_0)_2 (G_0)_3 C_0/G_0 (C_0)_5$
	C_{45}/G_0	$(C_0)_4 G_0 C_{45}/G_0 (C_0)_5$
Adhesive film	$C_0/adh./C_0$	$(C_0)_6/adh./(C_0)_6$
	$C_0/adh./C_{45}$	$(C_0)_4 C_{45} C_0/adh./C_{45} (C_0)_5$

2.2. Static mode I test procedure

Specimen are tested in pure mode I using Double Cantilever Beam tests. Dimensions of DCB specimens are given in Fig. 1. The pre-crack induced by the PTFE film is propagated up to 30 mm from the specimen border using an electromechanical tensile machine. The load is then released and the DCB test is carried out. Force, opening and crack length are measured during the test. The energy release rate is calculated using Eq. (1) [16].

$$G_{Ic} = \frac{3P\delta}{2B(a + |\Delta|)} \frac{F}{N} \quad (1)$$

where P is the load, δ the opening, B the width of the specimen, a the crack length, Δ a corrective term for the crack length, F and N two corrective terms to take into account the stiffening due to the presence of the end blocks [16].

2.3. Dynamic mode I test rig and procedure

So as to perform dynamic mode I tests, a specific test rig is designed and manufactured. The rig, presented in Fig. 2, consists in fixing the end blocks of the DCB specimen to a fixed frame at one side and a moving frame on the other side. By impacting the moving frame with a drop weight tower, the specimen is tested in mode I. The fixed frame is made of stainless steel whereas the moving frame is made of pultruded carbon fibers, to limit its weight. The crack length is monitored using a *Photron FastCam* high-speed camera at 30,000 fps. A load cell is placed between the specimen and the fixed frame to measure the crack propagation load. Finally the displacement of the moving frame is monitored using a unidirectional analogic displacement sensor.

The results are presented in Fig. 3. During a test, the crack propagates discontinuously. A first propagation phase is observable between 0 and 0.8 ms. The crack propagates at a constant velocity reaching 20–25 m/s. It is represented by the part (OA) of the graph. A second propagation phase is observable between 1.7 and 2.6 ms (corresponding to the part (BC) of the graph). The crack then propagates with a speed less than 10 m/s. Only the results obtained in the first propagation zone (noted [OA] in Fig. 3) are considered. This is the stable phase where the propagation velocity is regular and higher.

Increasing the impact velocity on the moving frame leads to an increasing in the intensity of the vibrations conducted by the frame and a barely readable signal. Furthermore, the crack propagates for the early displacements of the moving frame, where the moving frame velocity is not yet in a steady-state. Thus, it is compulsory to find a way to store some energy in the specimen before the crack propagation.

Using the work of Guo and Sun [13], a 15 mm wide adhesive tape is placed right after the end blocks to hold the specimen closed before the experiment. Right after the impact, the adhesive tape is stretched up to failure. The energy stored by the adhesive tape is instantly transmitted to the specimen, whom crack propagates at velocities reaching 100 m s^{-1} . This procedure has been proved to be very repeatable with variations on the crack propagation velocity of $\pm 5\%$ with the same experimental parameters. This procedure also produces very stable crack propagation.

To analyze the results of these experiments, the beam theory presented earlier in Eq. (1) is not relevant anymore. The simple energy method is used as a first approach. To be coherent between the quasistatic and dynamic fracture toughness measurements, the results from the quasistatic tests have been analyzed by both the beam theory and the energy method, and a maximum difference of 7% between the two measurements of G_{Ic} has been found. The beam theory proving to give more consistent results, it has been chosen to keep this method for the analysis of quasistatic tests.

For each configuration, 12 experiments are carried out at the same moving frame velocity of 4 m s^{-1} . Four specimens are tested without the adhesive tape, the others being tested with two 2 different lengths of adhesive tapes which allows tuning the crack propagation velocity. The crack speed obtained for the three configurations are respectively $20 \pm 3 \text{ m s}^{-1}$, $50 \pm 5 \text{ m s}^{-1}$ and $100 \pm 10 \text{ m s}^{-1}$.

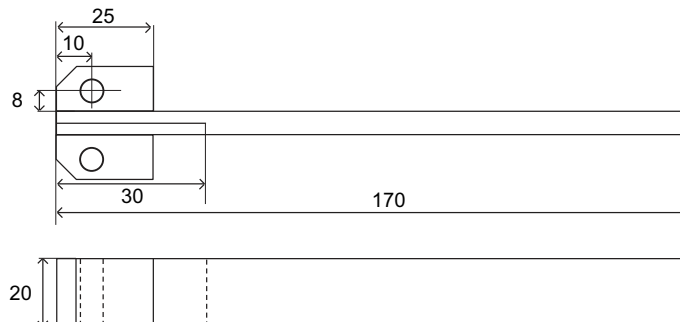


Fig. 1. Dimensions of DCB specimens and experimental set-up.

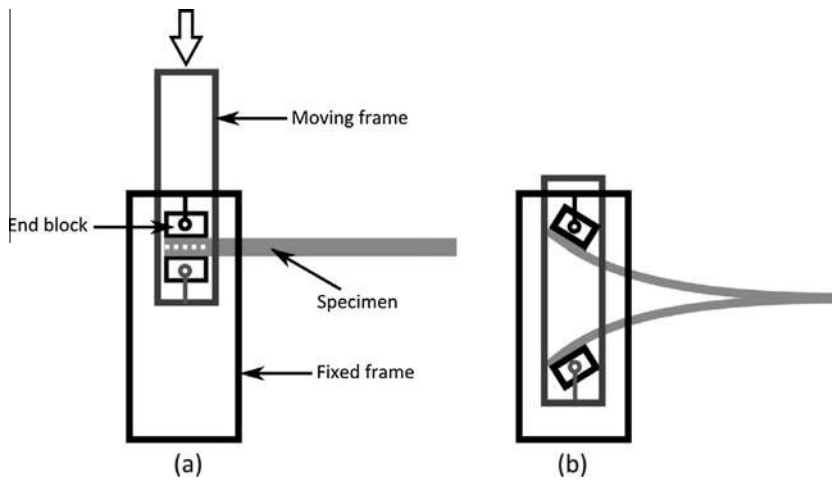


Fig. 2. Principle of the dynamic mode I test rig (a) before experiment; (b) after experiment.

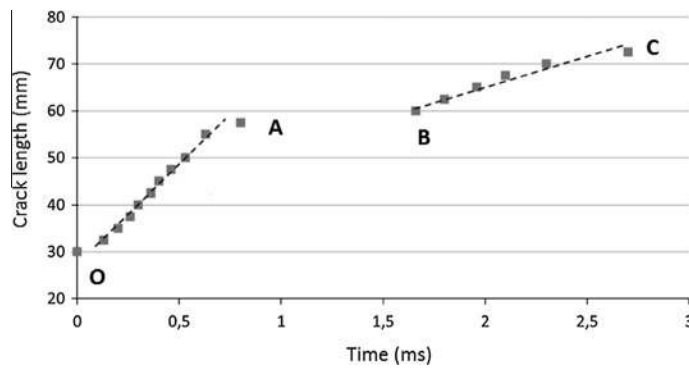


Fig. 3. Two regimes of the crack propagation.

2.4. Fractography

For each configuration, the specimens are cut after delamination from 10 mm to 20 mm from the initial pre-crack position. We consider that this zone is a stable state crack propagation zone that is representative of the whole specimen.

A gold film is deposited on each side of the delaminated specimen and each side is systematically observed using a Scanning Electron Microscope.

3. Delamination of woven laminates

All the results of this study are normalized by the energy release rate of the $C_0//C_0$ configuration. The average value of G_{Ic} measured for this configuration is 728 J/m^2 .

3.1. Preliminary observations

A microscopic view of the shape of the crack (Fig. 4) illustrates that in woven fabrics, the crack follows the shape of the tows and can bifurcate on each side of the tow. This phenomenon is found for all the configurations.

Fracture surface for $C_0//C_0$ specimens tested in mode I is given in Fig. 4. The specimen tested in mode I exhibits a clean fracture surface with fiber/matrix failure [17].

3.2. Influence of the woven fabric ply orientation

Fig. 5 shows the results of the study of the influence of woven fabric plies orientation on the critical energy release rate in mode I. The error bars give the standard deviation of the experimental results. The variations between the different results of the same configuration are low enough compared with the variations between the different configurations. The values of the

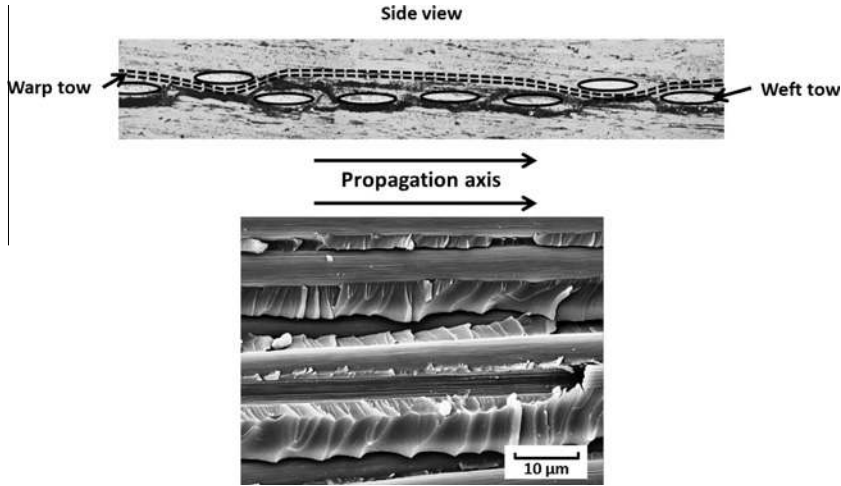


Fig. 4. Crack propagation shape and mode I fracture surface for the C_0/C_0 configuration.

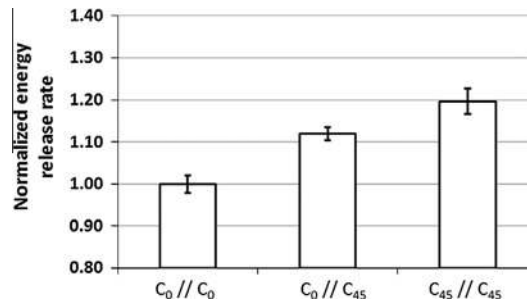


Fig. 5. Influence of the woven fabric ply orientation.

energy release rates are significantly higher (+10/+20%) for configurations with a woven fabric ply oriented at 45° with the propagation axis. Scanning Electron Microscope (SEM) pictures of the fracture surfaces of the C_0/C_0 and C_{05}/C_{45} configurations are given in Fig. 6. For the C_0/C_0 interface a clean fiber/matrix decohesion is observed whereas the C_{45}/C_{45} interface exhibits a rougher matrix failure surface. Fig. 6a and c reveals the apparition of resin pockets at the warp/weft intersection, especially for the C_{45}/C_{45} interface.

3.3. Influence of the material

Fig. 7 shows the results of the study of the influence of the nature of the fibers on the critical energy release rate in mode I. The values of the energy release rates are significantly higher (+10/+20%) for interfaces with one or two glass woven fabric plies compared to the pure carbon fabric interfaces. SEM pictures of the fracture surfaces of the C_0/C_0 and G_0/G_0 configurations are given in Fig. 7. For the C_0/C_0 interface a clean fiber/matrix decohesion is observed, whereas for the G_0/G_0 interface, pieces of matrix remain on the fibers.

3.4. Addition of an adhesive film

Fig. 8 shows the results of the study of the influence of the addition of an adhesive film on the critical energy release rate. The values of the energy release rates are significantly higher (+30/+50%) for interfaces with an adhesive layer compared with the same configurations without adhesive layer. SEM pictures of the fracture surfaces of the C_0/C_0 and $C_0/adh./C_0$ configurations are given in Fig. 8. Adding an adhesive layer intensifies fiber failure and fiber pull-out. These mechanisms can contribute to the higher values of energy release rates for these configurations, along with the higher toughness of the adhesive compared to the raw resin.

3.5. Influence of the crack propagation velocity

All the configurations are tested using the specific rig developed at the laboratory.

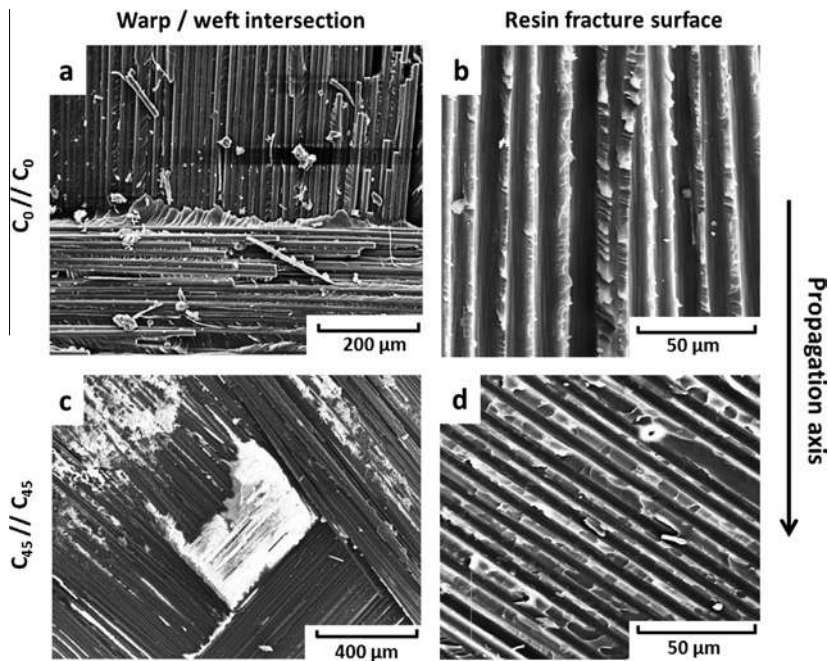


Fig. 6. Scanning electron microscope view of the fracture surfaces for different woven fabric ply orientation.

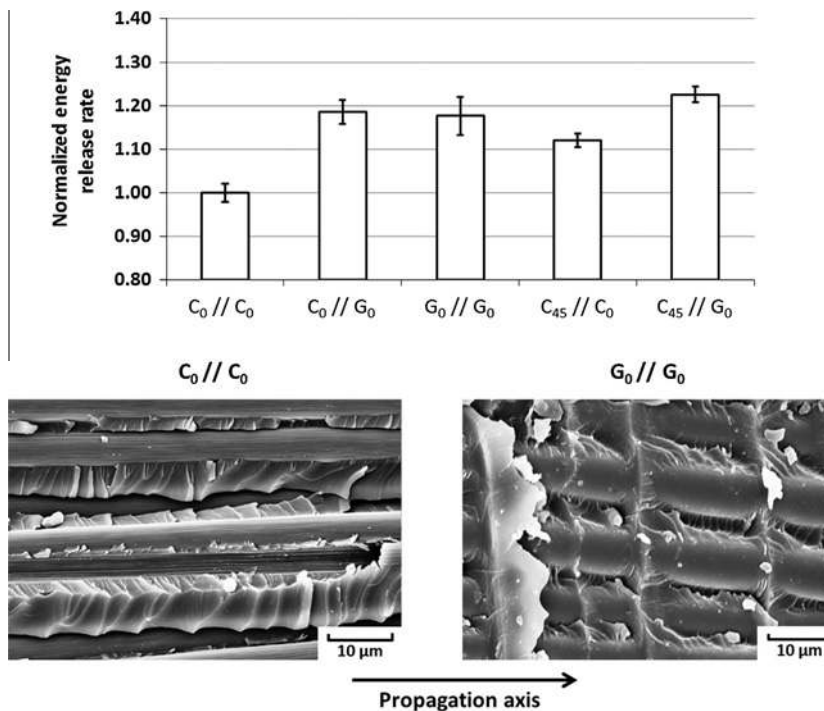


Fig. 7. Energy release rate and SEM views of the fracture surfaces for carbon and glass woven fabrics.

The influence of the crack propagation speed for the $C_0//C_0$ configuration is given in Fig. 9. Each point represents the average fracture toughness extracted from one experiment. Each error bar represents the standard deviation for each experiment. This result illustrates that the evolution of the fracture toughness for this configuration with the crack speed ranges within $\pm 15\%$ of the quasistatic value and that no tendency can be extracted. The fractographic study shows no differences in the separated surfaces of the specimen, except a cleaner resin failure (see Fig. 9). The same study on the other

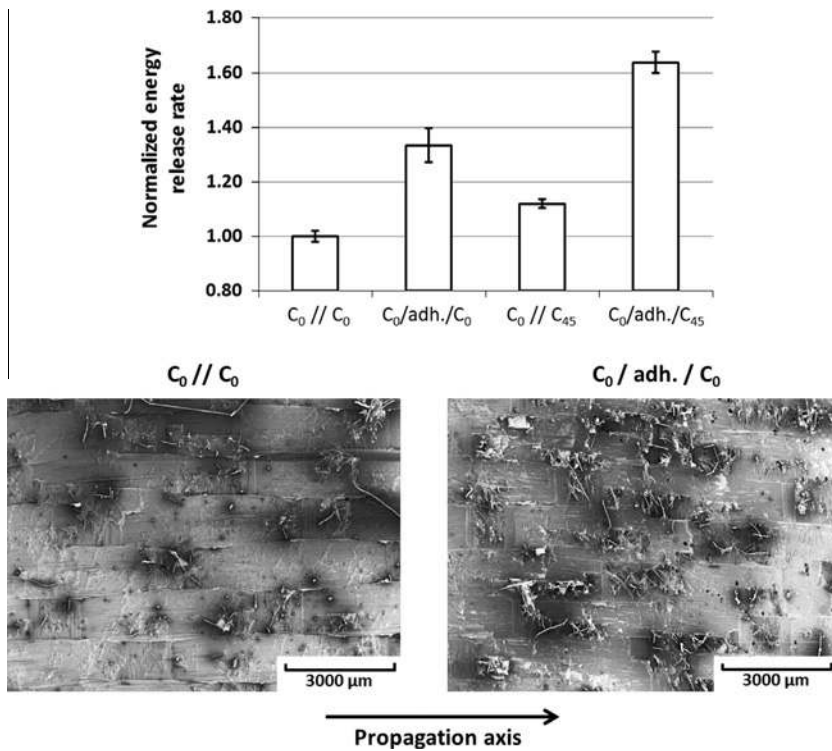


Fig. 8. Energy release rates and scanning electron microscope view of the fracture surfaces for carbon woven fabric without and with adhesive.

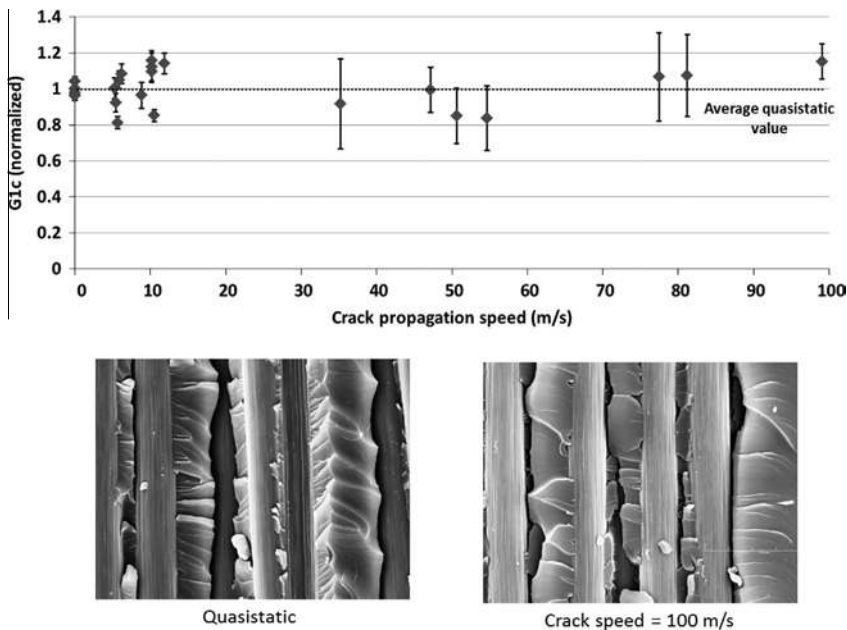


Fig. 9. Influence of the crack propagation speed on the fracture toughness and fractography for the C_0/C_0 configuration.

configurations is made and the summary of all the results is presented in Fig. 10. All the results are normalized compared to the quasistatic average fracture toughness. The error bars represents the minimum and the maximum values of the fracture toughness for each configuration and each speed. As for the C_0/C_0 configuration presented earlier, the evolution of the fracture toughness for the dynamic experiments is limited compared to the repeatability of the experiments.

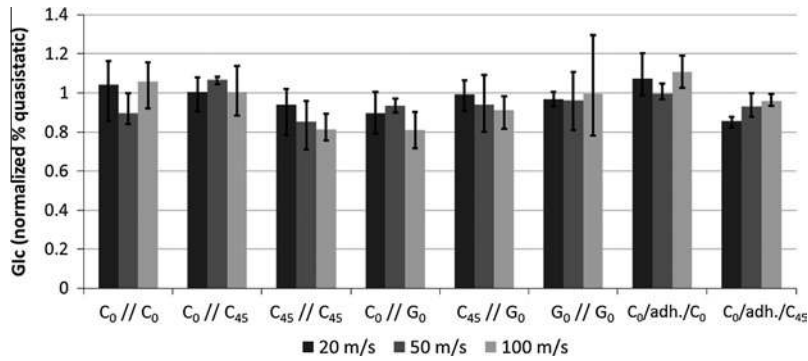


Fig. 10. Influence of the crack propagation speed on the fracture toughness.

4. Discussion

4.1. Damage mechanisms

The study of all the interfaces brought to light several damage mechanisms leading to delamination in woven laminates.

For each configuration a resin rich side and a clean fiber side are obtained, which is a classical phenomenon in woven composites [4]. The crack thus propagates mainly through the matrix. The phenomenon is particularly pronounced for the carbon woven fabric where the weak fiber/matrix cohesion causes the crack to propagate around the fibers, which leave a clean indent in the resin. Comparatively, the glass woven fabric presents a stronger fiber/matrix cohesion and exhibits a rougher fracture surface and a higher energy release rate.

For both these composites, the matrix is a 913 epoxy resin and the difference in behavior does not come from the matrix itself. The nature of the fibers is not enough to explain the differences in the behavior of the two materials with regard to the fiber/matrix strength. It has notably been shown that fiber surface treatment is an important parameter when considering delamination [18] and can improve the critical energy release rate by a magnitude of 2 [19]. Fiber coating could partially explain the differences between the glass and the carbon fabrics delamination toughness.

It has been shown that the addition of an adhesive film enhances the fiber failure and fiber pull-out phenomena and may even cause fiber bridging, a phenomenon classically minor in woven fabrics composites. In addition, the adhesive provides a tougher media for the crack to propagate through, which increases the energy release rate.

4.2. Orientation of the plies

Fig. 11 presents an explanation for the mechanisms leading to the crack propagation for the $C_0 // C_0$ and the $C_{45} // C_{45}$ interfaces. These mechanisms are derived from the work of Kim and Sham [5] on plain weave woven fabrics.

Due to the waviness of the woven fabric, each warp/weft tows intersection acts like an obstacle for the crack propagation. For the $C_{45} // C_{45}$ interface, the crack front encounters more of these intersections than for the $C_0 // C_0$ interface, as illustrated in Fig. 11. Moreover, the fibers are considered to provide a guide to the crack propagation [5,8]. For the $C_{45} // C_{45}$ interface, the propagation is off the axis of the fibers and more energy is needed to propagate the crack.

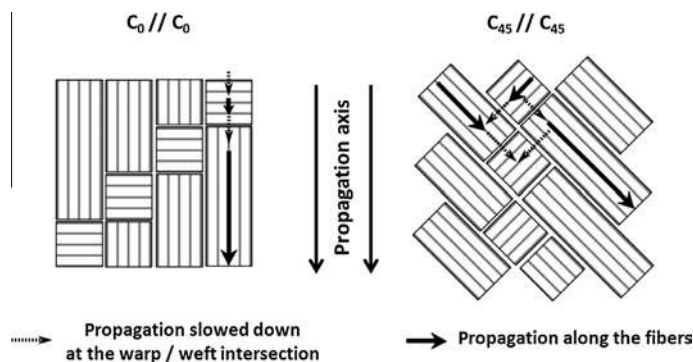


Fig. 11. Crack propagation for the $C_0 // C_0$ and the $C_{45} // C_{45}$ configurations.

4.3. Influence of the crack propagation speed

It has been shown that for the configurations tested in this study, there was no evidence of the influence of the crack propagation speed on the value of fracture toughness in mode I, in the velocity range [0–100 m/s]

This result has already been found for the unidirectional composites by the studies cited in the introduction as well as Tsai et al. [20]. The latter explains that this phenomenon can be explained by the Yang model [21] that links the fracture toughness, the stress intensity factor as well as the crack propagation speed. This law predicts an exponential increase in the fracture toughness for crack propagation speed higher than 1000 m/s. There would thus be a critical crack velocity, close to the speed of sound in the resin and far from the velocities tested in this study, for which the fracture toughness of the interfaces increase by 3–5 times their quasistatic value [22].

Although this law is hard to verify experimentally due to the complexity to measure a fracture toughness at such a high crack speed, it can confirm that the results obtained in this study for all the configurations are coherent.

5. Conclusions

In this article, the influence of several parameters (ply orientation, fiber nature and adhesive) on the delamination resistance of woven fabric composites has been studied. Each interface has been tested both in static and dynamic mode I using the DCB test and a specific rig.

The results have shown that orienting the plies off the axis of the fibers can increase the energy release rate in mode I and II by 10–20% compared with a 0°/0° configuration. SEM pictures of the delaminated surfaces have shown that for plies oriented at 45°, the crack front comes upon more warp/weft intersections and does not benefit from the guide provided by the fibers.

The study of interfaces with carbon and glass woven fabrics as well as with an adhesive layer at the interface has revealed the damage mechanisms leading to the delamination, notably the matrix and fiber/matrix failure, as well as the fiber failure and fiber pull-out for the composites with the higher energy release rates. The measurement of the dynamic fracture toughness of the different interfaces has shown no noticeable variations at the crack velocities tested. This result is coherent with previous studies on unidirectional materials. This work presents an experimental study in static and dynamic mode I via a rig specifically designed for dynamic delamination. The several configurations of woven fabrics tested in this study are seldom treated in the literature and offers a good comprehension of the good behavior of woven fabrics regarding delamination. The fractographic study realized for each of the interfaces tested have also allowed linking the values of the energy release rate with the damage mechanisms at the scale of the weaving pattern.

References

- [1] Abrate S. *Impact on Composite Structures*. Cambridge University Press; 2005.
- [2] Pereira AB, de Moraes AB, de Moura MFSF, Magalhães AG. Mode I interlaminar fracture of woven glass/epoxy multidirectional laminates. *Compos A Appl Sci Manuf* 2005;36(8):1119–27.
- [3] Funk JG, Deaton JW. *The interlaminar fracture toughness of woven graphite/epoxy composites*. NASA; 1989.
- [4] Kessler M, White S. Self-activated healing of delamination damage in woven composites. *Compos A Appl Sci Manuf* 2001;32(5):683–99.
- [5] Kim J-K, Sham M-L. Impact and delamination failure of woven-fabric composites. *Compos Sci Technol* 2000;60(5):745–61.
- [6] de Moraes A, de Moura M, Gonçalves JP, Camanho P. Analysis of crack propagation in double cantilever beam tests of multidirectional laminates. *Mech Mater* 2003;35(7):641–52.
- [7] de Moraes AB. Double cantilever beam testing of multidirectional laminates. *Compos A Appl Sci Manuf* 2003;12(34):1135–42.
- [8] Alif N, Carlsson LA, Boogh L. The effect of weave pattern and crack propagation direction on mode I delamination resistance of woven glass and carbon composites. *Compos B Engng* 1998;29(5):603–11.
- [9] Kusaka T, Hojo M, Mai Y-W, Kurokawa T, Nojima T, Ochiai S. Rate dependence of mode I fracture behaviour in carbon-fibre/epoxy composite laminates. *Compos Sci Technol* 1998;58(3–4):591–602.
- [10] Sun C, Han C. A method for testing interlaminar dynamic fracture toughness of polymeric composites. *Compos B Engng* 2004;35(6–8):647–55.
- [11] Hug G, Thevenet P, Fitoussi J, Baptiste D. Effect of the loading rate on mode I interlaminar fracture toughness of laminated composites. *Engng Fract Mech* 2006;73(16):2456–62.
- [12] Colin de Verdier M, Skordos AA, Walton AC, May M. Influence of loading rate on the delamination response of untufted and tufted carbon epoxy non-crimp fabric composites/Mode II. *Eng Fract Mech* 2012;96:1–10.
- [13] Guo C, Sun CT. Dynamic Mode-I crack-propagation in a carbon/epoxy composite. *Compos Sci Technol* 1998;58(9):1405–10.
- [14] Davidson BD, Krüger R, König M. Effect of stacking sequence on energy release rate distributions in multidirectional DCB and ENF specimens. *Eng Fract Mech* 1996;55(4):557–69.
- [15] Boeman R, Erdman D. *A practical test method for mode I fracture toughness of adhesive joints with dissimilar substrates*. Oak Ridge (Tennessee): Oak Ridge National Laboratory Engineering Technology Division.
- [16] Williams JG. Large displacement and end block effects in the 'DCB' interlaminar test in Modes I and II. *J Compos Mater* 1987;21(4):330–47.
- [17] Blackman BRK, Kinloch AJ, Paraschi M. The determination of the mode II adhesive fracture resistance, GIIC, of structural adhesive joints: an effective crack length approach. *Eng Fract Mech* 2005;72(6):877–97.
- [18] Albertsen H, Ivens J, Peters P, Wevers M, Verpoest I. Interlaminar fracture toughness of CFRP influenced by fibre surface treatment: Part 1. Experimental results. *Compos Sci Technol* 1995;54(2):133–45.
- [19] Varelidis PC, McCullough RL, Pappaspyrides CD. The effect on the mechanical properties of carbon/epoxy composites of polyamide coatings on the fibers. *Compos Sci Technol* 1999;59(12):1813–23.
- [20] Tsai JL, Guo C, Sun CT. Dynamic delamination fracture toughness in unidirectional polymeric composites. *Compos Sci Technol* Jan. 2001;61(1):87–94.
- [21] Yang W, Suo Z, Shih CF. Mechanics of dynamic debonding. *Proc Math Phys Sci* 1991;433(1889):679–97.
- [22] Tran AT. *Etude du délaminage en mode II de composites unidirectionnels soumis à des sollicitations rapides: approche globale et approche locale*. Paris: Ecole Nationale Supérieure d'Arts et Métiers; 2011.